Titin-Based Modulation of Calcium Sensitivity of Active Tension in Mouse Skinned Cardiac Myocytes Materials and Methods Preparations and Solutions

Olivier Cazorla, Yiming Wu, Thomas Irving, Henk Granzier

TITIN-BASED MODULATION OF CALCIUM-SENSITIVITY OF ACTIVE TENSION IN MOUSE SKINNED CARDIAC MYOCYTES.

(Titin and length-dependence of activation)

Olivier Cazorla*, Yiming Wu*, Thomas C. Irving and Henk Granzier.

OC, YW, HG: VCAPP , Washington State University, Pullman, WA, 99164-6520

TI: CSRRI, BCPS , Illinois Institute of Technology, Chicago, Illinois 60607-7171

* Authors contributed equally. OC's present address: Inserm U390/IFR3, Physiopathologie Cardiovasculaire, 34295 Montpellier cedex 05, France

HG: Corresponding author (Fax: (509)-335-4650 E-mail: granzier@wsunix.wsu.edu)

Abstract

We studied the effect of titin-based passive force on the length-dependence of activation of cardiac myocytes, in order to explore whether titin may play a role in the generation of systolic force. Force-pCa relations were measured at sarcomere lengths (SLs) of 2.0 and 2.3 μm. Passive tension at 2.3 μm SL was varied from ~1 to ~10 mN/mm^2 by adjusting the characteristics of the stretch imposed on the passive cell prior to activation. Relative to 2.0 μm SL, the force-pCa curve at 2.3 μm SL and low passive tension showed a leftward shift (ΔpCa_{50}) of 0.09 ± 0.02 pCa units while at 2.3 μm SL and high passive tension the shift was increased to 0.25 ± 0.03 pCa units. Passive tension also increased ΔpCa_{50} at reduced interfilament lattice spacing achieved with dextran. We tested whether titin-based passive tension influences the interfilament lattice spacing by measuring the width of the myocyte and by using small-angle X-ray diffraction of mouse LV wall muscle. Cell width and interfilament lattice spacing **varied inversely** with passive tension, in the presence and absence of dextran. The passive tension effect on length-dependent activation may therefore result from a radial titin-based force that modulates the interfilament lattice spacing..

Key words: X-ray diffraction, myofilament lattice, collagen, Frank-Starling.

Introduction

The precise mechanisms by which the heart is able to enhance its contractile performance in response to an increase in volume (Frank-Starling mechanism (FSM)) remain to be resolved. The cellular basis of the FSM involves the sarcomere length (SL) dependence of the Ca^{2+} sensitivity of tension[1]. Length-dependent Ca^{2+} sensitivity is revealed by the leftward shift of the force-pCa (-log[Ca^{2+}]) relation as SL is increased. The mechanisms that underlie this shift may involve **a length-dependent increase in affinity of the regulatory site of troponin C for Ca^{2+}**, as well as an increase in the number of strong binding cross-bridges[2,3]. The enhanced active force response when muscle is stretched may be explained by the myofilaments moving closer together[4], thereby increasing the probability of cross-bridge binding to actin[5,6]. Experiments in which the Ca^{2+} sensitivity was increased by osmotically compressing the filament spacing [5,6] support the idea that changes in myofilament spacing contribute to length-dependent activation.

Recent studies identified titin **(connectin)** as a possible factor involved in length-dependent Ca^{2+} sensitivity[7,8]. **The I-band segment of titin functions as a molecular spring that underlies the passive force of cardiac myocytes[9,10]**. This force is the main contributor to overall passive force of cardiac muscle, except towards the upper limit of the physiological SL range where collagen dominates[9,11]. **A passive force-based increase in the number of crossbridges bound to actin** has been suggested by earlier work on insect flight muscle[12] and rabbit psoas muscle[13]. Here we investigated the involvement of titin-based passive tension in the SL-dependence of Ca^{2+} activation of skinned cardiac myocytes and in modulating the interfilament lattice spacing. Force–pCa curves were measured at SL 2.0 μm and 2.3 μm and the pCa_{50} (pCa at half-maximal activation, an index of Ca^{2+} sensitivity) was determined at various levels of passive tension achieved by varying the stretch characteristics imposed on the cell prior to activation. We found that passive tension significantly influences both the length-dependence of activation and the **myofilament lattice spacing in normal and compressed muscle. Thus, titin is not just a passive spring that is independent of active force development, as is the conventional view, but titin also influences actomyosin interaction, possibly via modulating interfilament lattice spacing.**

Material and Methods

Preparations and solutions. Myocytes and muscles were isolated from mice and skinned as previously described [11,14]. Solution composition was as described [8] and all contained protease inhibitors[9]. For osmotic compression, dextran (T500) was used. . For additional details see Methods on-line.

Experimental set-up. The set-up was as described[11]. SL was measured on-line at 15 Hz (Ionoptix Corp., Milton Ma). The system uses a pseudo 2-D FFT analysis of the digitized striation images of the attached cell [15]. SL could be controlled during activation via adjusting the motor input voltage so as to keep SL at a constant value. Force was normalized by the cell's cross-sectional area (see [9]). The force-pCa relationship of freshly isolated cells was measured at 2.0 μm SL and then at 2.3 μm (15° C). Passive force was varied as explained below. Active forces at sub-maximal activations were normalized to that produced at pCa 4.5 at the same SL. (Force at pCa 4.5 slightly diminished with the number of imposed contractions; the mean reduction during the measurement of two force-pCa curves was **23 ± 2% (n=41**.)) The relationship between relative force and pCa was fitted to the equation: force = $[Ca^{2+}]^{nH} / (K + [Ca^{2+}]^{nH})$, where n_H is the Hill coefficient and pCa_{50} is $-(\log K)/n_H$). Values in Table 1 are the average values from all cells studied under a certain condition. All shown curves were fitted to the average force produced at each pCa.

X-ray Diffraction. The BioCAT undulator based beamline, Argonne National Laboratory was used. Muscles were mounted to a force transducer and a motor in a small trough with windows for collection of X-ray patterns and viewing of striations (SL was determined as described above). X-ray patterns were collected and spacings of the 1,0 and 1,1 equatorial reflections were measured and converted to $d_{1,0}$ values. For details see[4].

Titin degradation. X-ray experiments were performed on skinned muscle preparations that had been trypsinized (0.25 μg/ml; 25 min at 25 ˚C) to degrade titin[10,11]. To determine the amount of intact titin, preparations were solubilized after completion of the X-ray experiment and analyzed with SDS-PAGE. For details, see [9,16].

Statistics. Results are shown as the mean ± SE (unless indicated otherwise). Significant difference were assigned using the paired or unpaired Student's t test (as appropriate) or one way ANOVA and Tukey's multiple comparison with $P< 0.05$.

Methods On Line

Preparations and solutions. Myocytes and muscles were isolated from the left ventricular wall of 10-12 week old mice (Balb/C) as previously described[1,2]. For composition of relaxing (pCa 9) and maximal activating (pCa 4.5) solutions, see[3]. Intermediate pCa values were obtained by mixing these solutions in ratios as determined by the Fabiato program[4]. For osmotic compression, dextran (T500, Amersham Pharmacia) was used. Solutions contained protease inhibitors[5].

Experimental set-up. The set-up was as described[2]. Sarcomere length (SL) was measured on-line at 15 Hz (Ionoptix Corp., Milton, Ma). The system uses a pseudo 2-D FFT analysis of the digitized striation images of a region (32 horizontal pixel lines maximum) that encompasses most of the attached cell [6]. SL could be controlled during activation via manually adjusting the motor input voltage so as to keep SL (displayed on a computer screen) at a constant value. Forces were normalized by the cross-sectional area (measured from the imaged cross-section, see [5]). **Cells were activated via a perfusion pipette positioned near the cell. On occasion a slight drift occurred in the position of the pipette during the course of an experiment and this resulted in a minor difference in the speed of force development during activation (as may have occurred in Figure 2A; compare left and right panels).** For each cell, the force-pCa relationship was measured first at 2.0 and then at 2.3 μm SL (at 15° C). Passive force was varied as explained in the Result section. Active forces at sub-maximal activations were normalized to that produced at pCa 4.5 at the same SL. (The maximal active force at pCa 4.5 slightly diminished with the number of imposed contractions; the mean reduction during the measurement of two force-pCa curves was **23 ± 2% (n=41**.) The relationship between relative force and pCa was fitted to the equation: force = $[Ca^{2+}]^{nH}$ / (K + $[Ca^{2+}]^{nH}$), where n_H is the Hill coefficient and pCa_{50} is –(log K)/n_H). Values in Table 1 are the average values from all cells studied under a certain condition. The curves in Fig 2B, 2D and 4B were fitted to the average force produced at each pCa.

In some experiments we measured the cell widths using a 250 X magnification (100X objective (NA: 1.4) and a second optical magnification step of 2.5 X). Cell widths were determined from digitized images (pixel resolution 0.15 μm).

Measurements were made every 4 µm along the cell length and results in the central 1/3 of the cell were averaged.

X-ray Diffraction. The experimental arrangement was as described[7]. Briefly, the X-ray source was the BioCAT undulator based beamline, Argonne National Laboratory. Muscles were mounted to a force transducer and a motor in a small trough with windows for collection of X-ray patterns and viewing of striations. SL was measured immediately before and after the X-ray exposure by the multiple, pseudo 2-D FFT analysis technique similar to that described above. During the experiment, relaxing solution (at 15 ˚C) was pumped through the chamber. X-ray patterns were collected on a CCD-based X-ray detector and spacings of the 1,0 and 1,1 equatorial reflections were measured and converted to $d_{1,0}$ values using Bragg's Law.

Titin degradation. X-ray experiments were performed on skinned muscle preparations that had been trypsin treated to degrade titin (0.25 µg trypsin/ml at 25 ˚C for 25 min)[2,8]. Trypsin is a proteolytic enzyme that splits peptide bonds on the carboxyl side of lysine and arginine. Within the extensible region, the PEVK segment appears most prone to degradation, probably as a result of its disordered conformation (which promotes accessibility for trypsin), and its high lysine content. To determine the amount of intact titin, all preparations were solubilized after completion of the X-ray experiment and analyzed with SDS-PAGE and silver staining. For technical details, see [5,9].

To more completely determine the effect of trypsin on thin and thick-filament based proteins control and trypsin-treated muscle samples were pooled (~15 preparations each) quick frozen and then solubilized. Protein samples were loaded on gels at a range of volumes. Following electrophoresis and coommassie blue staining, gels were analyzed. The integrated OD of the protein peaks was determined and plotted against the loading volume. The linear part of the relations were fitted with a line and their slope determined. The slope ratio of the protein of interest versus MHC was then calculated. The analyzed proteins are shown in Fig. 5B (MyBP-C: myosin binding protein C; TnT: troponin T, TnI: troponin I; TnC: troponin C; LC1: myosin light chain 1; LC2: myosin light chain 2).

To determine the effect of trypsin on passive force developed by titin, collagen and intermediate filaments (IFs) we used a KCl/KI extraction of skinned cardiac muscle and myocytes (the preparations were perfused with 0.6 M KCl added to relaxing solution and then with 1 M KI in relaxing solution (cells: 10 min each; muscle: 45 min each). **This extraction removes thin and thick filaments and abolishes thereby titin as passive force generator, while collagen's force is unaffected[2]. The KCl/KI sensitive tension of muscle/cells is derived from titin and the KCl/KI insensitive tension from intermediate filaments (IFs) plus collagen in muscle (Fig. 5C) and IFs in myocytes (Fig. 5D) (The IF component is negligible at short SLs where collagen was studied. IFs were therefore ignored in the analysis of Fig. 5C). In some experiments we dissected small collagen strips from the myocardium and examined its force – length relation before and after trypsin treatment (Fig. 5E). Passive tension in Figs. 5C-E was measured with a slow ramp-like stretch with velocity 0.1 length/sec. In Fig. 5E the maximal SL was 2.25 µm for titin and muscle collagen, 3.5 µm for IFs. For collagen strips the maximal length was 120% of their resting length at zero force.**

We also measured the effect of trypsin-treatment on the force – pCa relation of muscle strips dissected from the LV free wall. Measurements were made at SL 1.9 µm and only one force-pCa curve was measured per preparation. Results are shown in Fig. 5F.

Calculation of repulsive and compressive force. The major repulsive force that separates myofilaments in skinned muscle (under relaxing conditions) is the electrostatic force (F_{ES}) that arises from the net negative charge carried by the thin and thick filaments (see Millman[7]). F_{ES} at the measured lattice spacings of Fig. 6A (control curve) were calculated based on numerical solutions to the Poisson-Boltzman equation (Equations 6 and 7 of Millman, B., and Nickel, B.[10] as implemented in the program MINIC, a FORTRAN program available from Dr. Irving) for a double hexagonal lattice of negatively charged rods. We assumed a charge radius of 13 nm for the thick filament and 4.5 nm for the thin filament with charge densities of 10 and 12 electrons/nm for the thick and thin filaments,

respectively (see[11]). This calculation yields a pressure in torr, which must then be converted to force/filament. To do this we assumed that electrically the thick filament can be represented as a cylinder of 13 nm in radius (the center of mass of heads) and 1.6 microns long i.e. 1.3^{-13} m^2 surface area. This implies that 1 torr electrostatic repulsive pressure is equivalent to 17 pN/filament.

As for the compressive force, in our model of Fig. 7A this force is derived from titin. Near the Z-line titin binds to the thin filament and at the A/I junction to the thick filament tip. Thus, the extensible region of titin is not parallel with the filaments but is under an angle (α, in Fig. 7A) and as a result titin's force (F) has a longitudinal (F_L) and radial component (F_r). F_L and F_r can be calculated from titin's total force (F) as F times cosα and F times sinα, respectively. The angle α was calculated from (1) the measured $d_{1,0}$ (Fig. 6A control) and converting this value to the thin-thick filament spacing (d_{10} times 2/3. See also [12]), and (2) the end-to-end length of titin's extensible region, obtained from our previous published measurements[13,14]. The obtained angles (in deg) ranged from 30 (SL 1.8 µm) to 8 (SL 2.25 µm). Measured titin-based tensions of mouse myocardium[2] were converted to force per half thick filament assuming that the fractional area of myofibrils is 0.7 [1] and calculating the number of thick filaments from the unit cell area based on the measured (Fig. 6A control) 43 nm d_{10} value at the slack length (area: d_{10} x d_{10} x 2/sqrt(3)= 2126 nm^2. Number of thick filaments per μm^2: 10^6 / 2126=470 thick filament μm^{-2}). The obtained force is the longitudinal force (F_L) of titin and this force was converted to (F_r) as F_L times sinα/cosα.

1. Cazorla O, Freiburg, A. , Helmes, M. , Centner, T. , McNabb, M. , Trombitás, K., Wu, Y., Labeit, S., and Granzier, H. Differential expression of cardiac titin isoforms and modulation of cellular stiffness. Circulation Research. 2000;86:59-67.
2. Wu Y, Cazorla, O., Labeit D., Labeit, S., Granzier, H. Changes in titin and collagen underlie diastolic stiffness diversity of cardiac muscle. Journal of Molecular and Cellular Cardiology. 2000;32:2151-2161.
3. Cazorla O, Vassort, G., Garnir, D., Le Guennec, J.-Y. Length modulation of active force in rat cardiac myocytes: is titin the sensor. Journal of Molecular and Cellular Cardiology. 1999;31:1215-1227.
4. Fabiato A. Computer Programs for Calculating Total From Specified Free or Free From Specified Total Ionic concentrations in Aqueous Solutions Containing Multiple Metals and Ligands. Methods in Enzymology. 1988;157:378-416.

5. Granzier HL, and Irving, T. C. Passive tension in cardiac muscle: contribution of collagen, titin, microtubules, and intermediate filaments. Biophys J. 1995;68:1027-1044.
6. Fan DS Wannenburg, T, and de Tombe PP. Decreased myocyte tension development and calcium responsiveness in rat right ventricular pressure overload. Circulation. 1997;95:2312-2317.
7. Irving T, Konhilas, J., Perry, D., Fischetti, R, and de Tombe, P. Myofilament lattice spacing as a function of sarcomere length in isolated rat myocardium. American Journal of Physiology/Heart Circulation Physiology. 2000;279:H2568-H2573.
8. Helmes M, Trombitas K, Granzier H. Titin develops restoring force in rat cardiac myocytes. Circ Res. 1996;79:619-626.
9. Granzier H, and Wang, K. Gel electrophoresis of giant proteins: solubilization and silver- staining of titin and nebulin from single muscle fiber segments. Electrophoresis. 1993;14:56-64.
10. Millman B, and Nickel, B. Electrostatic forces in muscle and cylindrical gel systems. Biophysical Journal. 1980;32:49-63.
11. Millman B. Irving, T. Filament lattice of frog striated muscle: radial forces, lattice stability, and filament compression in the A-Band of relaxed and rigor muscle. Biophys. J. 1988;54:437-447.
12. Irving thomas C. Millman, B. Z-line/I-band and A-band Lattices of intact frog sartorius muscle at altered interfilament spacing. Muscle Research and Cell Motility. 1992;13:100-105.
13. Trombitas K, Jin JP, Granzier H. The mechanically active domain of titin in cardiac muscle. Circ Res. 1995;77:856-61.
14. Granzier H, Helmes M, Trombitas K. Nonuniform elasticity of titin in cardiac myocytes: a study using immunoelectron microscopy and cellular mechanics. Biophys J. 1996;70:430-442.

Results

The Ca^{2+} sensitivity of active force was studied at various levels of passive force. To determine active force we subtracted the passive force prior to activation from total force during activation. However, this is only valid if during activation sarcomeres are isometric, since SL shortening reduces passive force and stretching has the opposite effect. We measured SL on-line and observed (as have others[6,8,15]) that although cells were kept isometric during contraction, sarcomeres typically changed length, especially when activation was maximal. The SL change varied somewhat from cell to cell, and for each cell we first performed a test contraction at pCa 4.5 and only continued with those cells that were well attached with minimal **(< 0.1 μm)** SL changes. When required, cell length was varied during contraction so as to keep SL constant (see Fig. 1). The differences in SL between the start and the peak of contraction of all cells used in this study **were** small (0.03 ± 0.02 μm). Thus, changes in passive force during contraction are negligible and active force equals the activation-induced force increase.

Passive force was adjusted by varying the SL history prior to activation. High levels of passive force were obtained by rapidly stretching the cell to 2.3 μm with activation following immediately (Fig. 1). Low to intermediate levels of passive force were obtained by (1) stretching sarcomeres to a length that exceeded 2.3 μm (typically to ~2.5 μm), (2) holding cell length constant, (3) releasing to 2.3 μm SL, and (4) holding the cell at 2.3 μm SL and then activating. The central panel of Fig. 2A shows an example of this protocol. During the hold phase at long SL (2), passive force rapidly decayed, most likely because of **contour length gain** of sub-domains within titin's extensible region[17]. **Recovery** takes place if the cell is completely released to the slack length and held there for several minutes. A partial release is insufficient for full refolding and passive force will therefore be lower[17]. These protocols allowed us to vary passive tension at SL 2.3 μm between ~1 and ~10 mN/mm^2.

When cells were sub-maximally activated at 2.3 μm SL, active force was significantly lower if passive force was low (compare Fig. 2A middle and right panels). This reduction in active force did not result from protocol-induced damage to either titin or the contractile apparatus as both passive and active forces recovered following a ~10-min rest period at the slack length (compare Fig 2A left and right panels). (To ensure that all contractions were induced at the same

passive force level, between contractions cells were always released to their slack length followed by a ~10 min rest and then imposing the exact same stretch – activation protocol.)

Force-pCa relationships were determined at 2.0 μm and 2.3 μm SL at high (8.7 ± 0.3 mN/mm^2) and low (1.7 ± 0.3 mN/mm^2) passive tension. At both passive tension levels the force-pCa curves at 2.3 μm were shifted leftward relative to the curve at 2.0 μm SL. The shift was significantly larger at high passive tension (Fig. 2B and Table 1). The pCa for half-maximal activation (pCa_{50}) increased by 0.25 ± 0.02 pCa units and 0.09 ± 0.01 pCa units for high and low passive tensions, respectively. Results were independent of the order in which the experiments were performed (high *vs*. low passive tension) indicating that no permanent damage was done by these protocols. **We measured the maximal active tension (pCa 4.5) in experiments in which three contractions were induced (in random order): (1) 2.0 μm SL, (2) 2.3 μm SL (low passive tension), and (3) 2.3 μm SL (high passive tension). Maximal active tensions (in mN/mm^2) were 30.7 ± 2.3 (n= 18), 31.6 ± 1.7 (n=13), and 34.3 ± 1.8 (n=18), respectively. Only results at 2.3 μm SL (high passive tension), were significantly higher than at SL 2.0 μm** (**ANOVA, $p<0.05$).**

Varying the amplitude and the duration of pre-stretch resulted in intermediate passive tension levels. Results from 29 cells were pooled in passive tension bins of 2.0 mN/mm^2 and their corresponding ΔpCa_{50} **(pCa_{50} at SL 2.3 minus pCa_{50} at 2.0 μm)** values were averaged. Fig. 2C shows that at passive tensions between 0-2 mN/mm^2, ΔpCa_{50} is 0.09 pCa units and that at higher tensions ΔpCa_{50} increases until it reaches 0.25 pCa units at a passive tension of 10 mN/mm^2. Linear regression (broken line in 2C) shows that the length dependence of activation (ΔpCa_{50}) has a passive tension independent component (~0.08 pCa units in size) and a component that varies with passive tension.

Considering that the large pre-stretch/partial release protocol requires stretch to non-physiological SLs, we also measured the force – pCa relation of cells in which passive tension was reduced with trypsin, as an independent method. Because of the high trypsin sensitivity of titin's PEVK domain, a mild trypsin treatment can be used to specifically degrade titin's I-band region and to lower thereby passive tension at a given SL[10,11] **(see also below and Methods on-line). Trypsin-treated cells were stretched to SL 2.3 μm and then**

immediately activated. Due to degradation of titin, passive tension was now low (1.7 ± 0.6 mN/mm^2; n=6). The force–pCa relation so obtained was shifted to the right compared to the curve measured at high passive tension (2D). The pCa_{50} (5.79 ± 0.04) and maximal active tension (33.1 ± 2.8 mN/mm^2) are indistinguishable from that at low passive tension obtained after the large prestretch/partial release protocol (5.78 ± 0.03, and 31.6 ± 1.7 mN/mm^2 respectively). Thus, reduction of passive tension via either trypsin treatment or a large stretch/partial release leads to the same force-pCa relation.

We studied whether the passive-tension induced shift of the force-pCa relation involves a passive tension effect on the myofilament lattice spacing as indicated by the cell width at 2.3 µm SL. Cell width was significantly smaller at high passive tension than at low passive tension (3C(a)). Furthermore, during stress recovery (Fig. 3C(b)) cells shrank significantly.

It is well known that the myofilament lattice spacing of striated muscles expands during skinning due to the loss of the osmotic constraint to swelling imposed by the sarcolemma [4,18,19]. It has been reported that the myofilament lattice upon skinning of cardiac muscle expands [19] and that this may be countered with ~2.5 % (w/v) dextran T-500. To test whether passive tension affects the length-dependence of activation in conditions where skinning-induced swelling was compensated, we measured the force-pCa relations at high and low passive tension in the presence of 2.5% dextran.

In the presence of dextran, the cell width at SL 1.9 µm was reduced by ~8% (Fig 4A), consistent with the 7-8% reduction reported by others [6,20]. The force-pCa relations at 2.0 µm SL in the presence of dextran were shifted to the left (relative to no dextran) to a position similar to the one obtained without dextran at 2.3 µm SL (Fig. 4B and Table 1). This is consistent with results of others obtained on cardiac myocytes[6] that showed that dextran sensitizes the cells at short SL. To our knowledge, the effect of dextran on the force-pCa relation of cardiac myocytes at 2.3 µm SL has not been investigated before. Relative to the curve at 2.0 µm SL (with dextran) our experiments revealed a ΔpCa_{50} of 0.08 pCa units at low passive tension and 0.15 pCa units at high passive tension (Figs. 4B and C, Table 1).

We measured the maximal active tension in experiments in which three maximal active contractions were induced: at SL 2.0 µm, SL 2.3 µm (low passive tension), and SL 2.3 µm

(high passive tension), in a randomized order. Maximal active tensions (in mN/mm^2) were 32.4 ± 2.5 (n= 10), 36.6 ± 2.3 (n=10), and 34.9 ± 2.0 (n=10), respectively. Results comparing high vs. low passive tension at 2.3 μm were not significantly different. The maximum tensions at 2.3 μm SL (low passive tension) and those at 2.3 μm SL (high passive tension) were both significantly higher than at 2.0 μm.

To further probe the mechanism underlying these findings we studied the effect of passive tension on myofilament lattice spacing, by using low-angle X-ray diffraction. Since X-ray diffraction on cells is currently not feasible, due to their low X-ray scattering mass, we used for these studies mouse skinned myocardium dissected from the left ventricular free wall. Figure 5A panel 1 shows a typical X-ray pattern from a skinned preparation in relaxing solution with clearly resolved equatorial reflections. (SDS-PAGE showed that titin was unaffected by the X-ray exposure.) The separation of these reflections allowed us to measure lattice spacing with ~0.1 nm resolution. Myofilament lattice spacing decreased significantly as SL was increased (Fig. 6A), consistent with recent measurements on rat cardiac trabeculae[4].

To vary passive tension we were unable to use the 'large pre-stretch protocol' as collagen in mouse myocardium limits the maximal SL with reversible mechanical characteristics to ~2.3 μm[11]. Again we varied passive tension by degrading titin with trypsin (0.25 μg trypsin/ml; 25 min at 25 ˚C). Treating mouse skinned myocardium with trypsin greatly degraded titin (T1) without significantly affecting other proteins (5B). To test whether trypsin affects collagen-based force we trypsin-treated collagen strips as well as myocardium that had been extracted with high salt to abolish titin as a source of passive force[11]. Collagen's force was unaffected by trypsin (5C and E). We also tested whether trypsin affects intermediate filament (IF) based force and found that also this force is not affected by trypsin (5D and E). **Finally, we measured the force-pCa relation at a SL of 1.9 μm and found that the relation was unaffected by trypsin (Fig. 5F). Neither pCa_{50} (control: 5.71 ±0.03 (n=12); trypsin treated: 5.73 ± 0.04 (n=12)) nor maximal active tension (control: 25.7 ± 2.0 mN/mm^2; trypsin treated: 23.3 ± 1.7 mN/mm^2 (n=12)) were significantly affected by trypsin. Thus, under our experimental conditions trypsin specifically abolishes titin-based passive force.**

An example of an X-ray diffraction pattern following trypsin treatment is shown in 5A panel 2 and the SL-dependence of the $d_{1,0}$ spacing before and after trypsin-treatment in 6A. Degradation of titin significantly increased the lattice spacing with an average increase of ~3 nm. **The large increase in $d_{1,0}$ at SL 1.9 µm and our finding that trypsin treatment does not affect calcium sensitivity at SL 1.9 µm (Fig. 5F) suggests that calcium sensitivity is independent of $d_{1,0}$ spacing in the ~44-47 nm range. Although support for the idea that changes in myofilament lattice spacing contribute to length-dependent activation [5,6] is compelling, this finding may be viewed as a cautionary note.**

We also studied whether degrading titin had an effect on the osmotically compressed lattice achieved by adding dextran. Definitive studies of the amount of dextran required to restore the *in vivo* lattice spacing in skinned cardiac muscle have not been reported, earlier studies used a range from 2 to 4% dextran[4,19,20], and we chose 4% for these experiments. An example of a X-ray pattern is shown in Fig. 5A panel 3 and the SL dependence of $d_{1,0}$ in 6B. Results indicate that at a given SL, dextran greatly reduces the lattice spacing. For example, at SL 2.1 µm dextran reduced $d_{1,0}$ from 42.4 nm to 35.4 nm. (Note that this spacing in dextran is close to that of intact cardiac muscle at SL 2.1 µm: for rat reported values are 34.8 nm[4] and 35.6 nm[19]). The effect of degrading titin with trypsin in the presence of dextran was then studied. An example of a X-ray pattern is shown in 5A panel 4 and measurements in 6B. Degrading titin significantly increased the lattice spacing, this increase being largest at 1.9 µm SL with a gradual decrease with SL. These studies support the notion that titin modulates the interfilament lattice spacing both in the presence and absence of dextran.

Discussion.

Numerous studies have shown that an important component of the Frank-Starling mechanism is the length-dependence of the calcium-sensitivity of force. A now widely held explanation for length-dependent activation is that the change in interfilament spacing that accompanies SL change modulates the probability of actomyosin interaction at the same calcium concentration. The mechanism by which interfilament spacing affects actomyosin interaction may involve an interfilament-spacing effect on weakly bound crossbridges by affecting their number [21] or the rate of transition from the weak to strong binding states[22]. Here we report that titin modulates interfilament spacing and that titin-based passive tension influences length-dependent activation.

Effect of titin-based passive tension on calcium sensitivity. Due to stress relaxation, titin-based passive tension at a given SL is not constant but decreases with time. We took advantage of the high degree of passive stress relaxation at long SL and its slow recovery upon partially releasing the cell, to vary passive tension at a SL of 2.3 μm and study its effect of the force-pCa relation. Results indicate that the length dependence of activation (ΔpCa_{50}) has a passive tension independent component of 0.08 pCa units (intercept of line in Fig. 2C) that is likely to involve thin and thick filament based processes independent of titin. The passive tension independent component is somewhat less than the ~0.12 ΔpCa_{50} values reported by other laboratories studying the mouse [23-25]. Although passive tension was not reported in these previous studies, they employed protocols generally consisting of a slow stretch followed by a long wait period prior to activation, and passive tensions are therefore likely to have been relatively low (our Fig. 2C indicates that a ΔpCa_{50} of 0.12 is accompanied by ~2.5 mN/mm^2 passive tension). Thus, the ΔpCa_{50} values at low passive tension found here are in general agreement with those of others. High passive tensions were achieved by rapidly stretching cells to SL 2.3 μm and then immediately activating (Fig. 1). We found that passive tension significantly enhances the length-dependence of activation with a ΔpCa_{50} of 0.25 pCa units at the highest passive tensions employed. Thus, for maximal calcium sensitivity of skinned cardiac myocytes, a high level of titin-based passive tension is required.

Effect of titin on interfilament spacing. For cardiac myocytes we used the cell width as an indicator of interfilament spacing. Although cell width is an imperfect indicator, it nevertheless

provides qualitative insights into myofilament lattice behavior[20]. We found that passive tension correlates negatively with cell width (Fig. 3) suggesting that titin modulates myofilament lattice spacing. In agreement with this are the low-angle X-ray diffraction studies on cardiac muscle that showed that degradation of titin significantly increases $d_{1,0}$. These findings are consistent with results on mechanically skinned skeletal muscle fibers where a close correlation is found between titin-based passive tension and $d_{1,0}$[26] and where following degradation of titin, $d_{1,0}$ is independent of SL[27]. Thus, titin is a modulator of interfilament lattice spacing in skeletal and cardiac muscle.

Following titin degradation, the myofilament lattice was still responsive to SL (Fig. 6). This suggests that in addition to titin other modulators of myofilament lattice spacing exist. A possible candidate is collagen. By comparing $d_{1,0}$ of chemically and mechanically skinned skeletal muscle fibers, it has been shown that at long SL collagen compresses the myofilament lattice in skeletal muscle[26]. In myocardium collagen is the main source of passive tension at long SL while titin is the main source at short SL[9,11]. If collagen and titin both affect lattice spacing, eliminating titin's force will have the largest effect on spacing at short SL and the smallest at long SL, giving rise to steeper $d_{1,0}$– SL relations following elimination of titin. This expectation is in agreement with our findings (Fig. 6) and supports the idea that the myofilament lattice spacing is under the influence of both collagen and titin.

The segment of titin near the Z-line binds strongly to the thin filament[28] and the A-band segment of titin attaches to the thick filament[29]. Thus the elastic region of titin runs obliquely to the thin and thick filaments, with an angle that depends on thin-thick filament spacing and on the end-to-end length of titin's extensible region (see Fig. 7A). As a result, titin is expected to develop a longitudinal force (F_L) and radial (F_r) force, the latter of which compresses the lattice **(7A, inset)**.

The major repulsive force that separates myofilaments in skinned muscle (under relaxing conditions) is the electrostatic force (F_{ES}) that arises from the net negative charge carried by the thin and thick filaments [18]. F_{ES} at the measured lattice spacings of Fig. 6A (control curve) were calculated as described in Methods on-line. Results shown in Fig 7B reveal that the repulsive force, F_{ES}, and the compressive component of titin-based passive force, Fr, are of similar magnitude. Thus, titin develops a radial force that is sufficiently

large for it to play a role in counteracting the repulsive F_{ES}, supporting the concept that titin can modulate the myofilament lattice spacing of passive muscle.

The proposal that titin gives rise to a radial force is consistent with the reduced effect of titin on myofilament lattice spacing in the presence of dextran (Fig. 6). Compressing the myofilament lattice increases the repulsive force between filaments[30] while the radial force will be reduced. The latter results from the more shallow angle adopted by the titin filament (α in Fig. 7A) when thin and thick filaments move closer together. Calculations show that the 6 nm $d_{1,0}$ reduction in dextran (control curves of Fig. 6) reduces F_r by ~15%. Thus, in the presence of dextran, titin's effect on myofilament lattice spacing is expected to be reduced, consistent with $d_{1,0}$ measurements (Fig. 6B) and the reduced effect of passive tension on ΔpCa_{50} (Fig. 4).

Our work suggests that titin-based passive force modulates the myofilament lattice spacing and it seems reasonable to propose that this underlies at least part of the effect of titin's passive force on the length dependence of calcium sensitivity. It is also possible that a role is played by an earlier proposed mechanism[12,13] in which crossbridge disorder is enhanced by passive force induced thick filament strain, which leads to an increased likelihood of actomyosin interaction and an increase in calcium sensitivity. The notion that the crossbridge order can vary in passive muscle is supported by studies that investigated thick filament structure in response to changes in passive stretch[31], temperature[32], phosphorylation of myosin light chains[33] and C-protein[34]. Thus, thick filament strain as well as interfilament spacing may be involved in linking titin to calcium sensitivity, and their relative importance and interrelationship remains to be established.

In conclusion, titin influences the length-dependence of calcium sensitivity of active force in cardiac myocytes and the underlying mechanism may involve an effect of titin on myofilament lattice spacing. These findings challenge the conventional notion that titin is independent of actomyosin-interaction and they suggest that titin has the potential to enhance systolic performance as the ventricular volume is increased.

Acknowledgements. We acknowledge Dr. deTombe and lab members for assistance and use of their mechanics set-up for X-ray work. Supported by HL67274 and HL62881(HG) AHA9950459N (TI) and an AHA fellowship to OC. Use of APS supported by Department of Energy (W-31-109-ENG-38). BioCAT is a NIH-supported Research Center RR08630.

Table 1: Effects of passive tension and dextran on calcium sensitivity.

		SL 2.0 μm			**SL 2.3 μm**			
Dextran	n	Passive tension (mN/mm^2)	pCa_{50}	n_H	passive tension (mN/mm^2)	pCa_{50}	n_H	ΔpCa_{50}
0%	10	0.5 ± 0.1	5.69 ± 0.02	3.1 ± 0.2	1.7 ± 0.3*	5.78 ± 0.03*	3.0 ± 0.2	0.09 ± 0.01*
0%	10	0.6 ± 0.1	5.64 ± 0.02	2.8 ± 0.2	8.7 ± 0.3	5.89 ± 0.02	3.4 ± 0.3	0.25 ± 0.02
2.5%	7	0.4 ± 0.1	5.92 ± 0.03	2.7 ± 0.2	2.2 ± 0.4*	6.01 ± 0.03*	2.9 ± 0.2	0.09 ± 0.01*
2.5%	7	0.5 ± 0.1	5.91±0.02	2.4 ±0.1	8.7 ± 0.9	6.06 ± 0.03	2.7 ± 0.2	0.15 ± 0.01

Number of cells: n. Hill coefficient: n_H. ΔpCa_{50}: pCa_{50} at SL 2.3 minus pCa_{50} at 2.0 μm (each cell functioned as its own control). * Significant difference between results at high vs. low passive tension.

CAPTIONS

Figure 1. **A)** Myocyte glued to force transducer (left) and motor (right) at SL 2.3 μm. Top: passive **(**pCa 9.0); bottom: active (pCa 4.5). During activation SL was kept constant by slightly stretching the cell. **B)** Force and SL of cell stretched from 2.0 to 2.3 μm in relaxing solution, held and maximally activated (pCa 4.5). At the beginning of contraction, SL was controlled. Apart from transients, SL changes are small.

Figure 2) Effect of passive force on activation. **A)** Top: schematic of SL change; bottom: force. Left and right panels: myocyte stretched from 2.0 to 2.3 μm SL and then Ca^{2+} activated. Middle panel: myocyte stretched to 2.5 μm SL (1), held (2), released to 2.3 μm SL (3), and held and activated at 2.3 μm SL (4). In middle panel both passive force at the start of activation and maximal active force were reduced. **B)** Average force-pCa relationship at 2.0 μm SL (■) and 2.3 μm with high passive tension (8.7 ± 0.3 mN/mm^2 ; ●) and low passive tension (1.7 ± 0.3 mN/mm^2; ❍). Note that curves at 2.3 μm SL are shifted leftwards and that this shift is largest at high passive tension. **C)** Effect of passive tension on ΔpCa_{50}. The broken line is the linear regression line fitted to the mean results. D) Force-pCa relationship at 2.0 μm SL and 2.3 μm with high passive tension (results from 2B) and low passive tension achieved by trypsin treatment of the cells.

Figure 3. Effect of passive force on cell width. A) Length change protocols. B) Examples of passive force responses. C) Cell width measurements immediately after completion of stretch/release and 5 min later. Pooled results at high (left panel) and those at low (right panel) passive tensions were significantly different (a). Results following 5 min of stress recovery (right panel) were significantly different (**Paired t-test: P=0.05)** from those immediately following release (b). **(Mean ± SE of 14 cells from 7 animals.)**

Figure 4. Effects of osmotic compression (2.5% dextran). A) Cell width is significantly reduced by dextran (shown are results before the addition of dextran, in the presence of dextran, and following dextran washout). B) Force-pCa curves in presence of dextran at 2.0 μm SL (■) and 2.3 μm SL at high (●) and low (❍) passive tension (8.7 ± 0.9 mN/mm^2 and 2.2 ± 0.3 mN/mm^2, respectively). (Right most curve is the relationship at SL 2.0 μm

from Fig. 2B). C) Relation between passive tension and ΔpCa_{50} (both measured in the presence of dextran) (The broken line is from Fig. 2C.)

Figure 5. **A**) X-ray patterns from skinned left ventricular wall muscle in relaxing solution (SL: 2.0 μm) showing strong equatorial reflections. 3 and 4: in the presence 4% dextran. 2 and 4: trypsin-treated. **B**) Relative content of titin (T_1) and thin and thick-filament based proteins. Only titin is significantly degraded by trypsin (n=6). **C**) **Length-tension relation of collagen of mouse muscle before (top) and after (bottom) trypsin treatment (n=5). D**) **Length-tension relation of intermediate filaments of mouse cardiac myocytes before (bottom) and after (top) trypsin treatment. E) Effect of trypsin on tensions of titin, muscle collagen, collagen strips, and intermediate filaments. Absolute control tension levels (in mN/mm^2) for titin 18.6 ± 1.9 (n=5), muscle collagen 24.4± 3.2 (n=5), collagen strips 18.2 ± 4.3 (n=5), and intermediate filaments 6.3 ± 3.0 (n=5).** F) Force–pCa relations of control mouse muscle (closed circles and broken line) and trypsin-treated muscle (open circles and solid line). *Denotes significant differences from control. **(See Methods on-line for details on how collagen, titin and IF forces were determined.)**

Figure 6. Effect of dextran and trypsin on myofilament lattice spacing of skinned muscle. Results of 10 preparations were binned in 0.05 μm SL intervals and the mean ± SE calculated. **A**) Measurements in absence of dextran of control and trypsin-treated muscle. **B**) Results in the presence of 4% dextran. Lines are linear regression lines. (Their slopes are indicated.)

Figure 7. Model of how titin modulates myofilament lattice spacing. **A**) Near the Z-line titin binds to the thin filament and at the A/I junction to the thick filament tip. Thus, the extensible region of titin is not parallel with the filaments**, and titin's force (F) has a longitudinal and radial component (F_L and F_r)**. **B**) Titin's radial force - SL relation and the inter-filament electrostatic repulsive force (F_{ES}) - SL relation. For details see text and Methods on-line.

References

1. Kentish JC. TerKeurs H., Ricciardi L., Bucx JJJ., Noble MIM. Comparison between the sarcomere length-force relations of intact and skinned trabeculae from rat right ventricle: influence of calcium concentrations. Circulation Research. 1986;58:755-768.
2. Metzger J. Myosin binding-induced cooperative activation of the thin filament in cardiac myocytes and skeletal muscle fibers. Biophysical Journal. 1995;68:1430-1442.
3. Wang Yi-Peng Fuchs F. Length, Force, and Ca^{2+}-Troponin C Affinity in Cardiac and Slow Skeletal Muscle. Am. J. Physiol. 1994;266:C1077-C1082.
4. Irving T, Konhilas, J., Perry, D., Fischetti, R, and de Tombe, P. Myofilament lattice spacing as a function of sarcomere length in isolated rat myocardium. American Journal of Physiology/Heart Circulation Physiology. 2000;279:H2568-H2573.
5. Fuchs F. Wang Y. Sarcomere Length Versus Interfilament Spacing as Determinants of Cardiac Myofilament Ca2+ Sensitivity and Ca2+ Binding. J. Mol. Cell Cardiol. 1996;28:1-9.
6. McDonald K, Moss, R. Osmotic compression of single cardiac myocytes eliminates the reduction in calcium sensitivity of tension at short sarcomere length. Circulation Research. 1995;77:199-205.
7. Cazorla O, Pascarel C, Garnier D, Le Guennec JY. Resting tension participates in the modulation of active tension in isolated guinea pig ventricular myocytes. J Mol Cell Cardiol. 1997;29:1629-1637.
8. Cazorla O, Vassort, G., Garnir, D., Le Guennec, J.-Y. Length modulation of active force in rat cardiac myocytes: is titin the sensor. Journal of Molecular and Cellular Cardiology. 1999;31:1215-1227.
9. Granzier H, and Irving, T. Passive tension in cardiac muscle: contribution of collagen, titin, microtubules, and intermediate filaments. Biophys J. 1995;68:1027-1044.
10. Helmes M, Trombitas K, Granzier H. Titin develops restoring force in rat cardiac myocytes. Circ Res. 1996;79:619-626.
11. Wu Y, Cazorla, O., Labeit D., Labeit, S., Granzier, H. Changes in titin and collagen underlie diastolic stiffness diversity of cardiac muscle. Journal of Molecular and Cellular Cardiology. 2000;32:2151-2161.
12. Granzier H, and Wang, K. Interplay between Passive Tension and Strong and Weak Binding Cross-Bridges in Insect Indirect Flight Muscle. J. Gen. Physiol. 1993;101:235-270.

13. Granzier H, and Wang, K. Passive tension and stiffness of vertebrate skeletal and insect flight muscles: the contribution of weak cross-bridges and elastic filaments. Biophys J. 1993;65:2141-59.
14. Cazorla O, Freiburg, A. , Helmes, M. , Centner, T. , McNabb, M. , Wu, Y., Trombitás, K. , Labeit, S., and Granzier, H. Differential expression of cardiac titin isoforms and modulation of cellular stiffness. Circulation Research. 2000;86:59-67.
15. Fan DS, Wannneburg T, and deTombe P. Decreased myocyte tension development and calcium responsiveness in rat right ventricular pressure overload. Circulation. 1997;95:2312-2317.
16. Granzier H, and Wang, K. Gel electrophoresis of giant proteins: solubilization and silver- staining of titin and nebulin from single muscle fiber segments. Electrophoresis. 1993;14:56-64.
17. Helmes M, Trombitas, K, Centner, T, Kellermayer, M, Labeit, S, Linke, A, and Granzier, H. Mechanically driven contour-length adjustment in rat cardiac titin`s unique N2B sequence: titin is an adjustable spring. Cir Res. 1999;84:1139-1352.
18. Millman BM. The filament lattice of striated muscle. Physiol Rev. 1998;78:359-91.
19. Matsubara I. Maughan D., Saeki Y, Yagi N. Cross-Bridge Movement in Rat Cardiac Muscle as a function of Calcium Concentration. Physiology. 1989;417:555-565.
20. Roos KP. Brady A. Osmotic compression and stiffness changes in relaxed skinned cardiac myocytes in PVP-4 and Dextran T-500. Byophys. J. 1990;58:11273-1283.
21. Smith S, and Fuchs, F. Length-dependence of cross-bridge mediated activation of the cardiac thin filament. Journal of Molecular and Cellular Cardiology. 2000;32:831-838.
22. McDonald K, Wolff, M., and Moss, R. Sarcomere length dependence of the rate of tension redevelopment and submaximal tension in rat and rabbit skinned skeletal muscle fibers. Journal of Physiology. 1997;501:607-621.
23. Wolska B, Keller, R., Evans, C., Palmiter, K., Phillips, R., Muthuchamy, M., Oehlenschlager, J., Wieczorek, D., de Tombe, P., Solaro, J. Correlation between myofilametn response to calcium and altered dynamics of contraction and relaxation in transgenic cells that express beta-tropomyosin. Circulation Research. 1999;84:745-751.
24. Arteaga G, Palmiter, K., Leiden, J., Solaro, J. Attenuation of length dependence of calcium activation in myofilaments of transgenic mouse hearts expressing slow skeletal troponin I. Journal of Physiology. 2000;526:541-549.

25. McDonald K, Field, LJ., Parmacek, MS., Soonpaa, MS., Leiden, JM. Moss, RL. Length dependence of Ca2+ sensitivity of tension in mouse cadiac myocytes expressing skeletal troponin C. Journal of Physiology. 1995;483:131-139.

26. Higuchi H, Umazuma Y. Lattice Shrinkage with Increasing Resting Tension in Stretched, Single Skinned Fibers of Frog Muscle. Biophysical Society. 1986;50:385-389.

27. Higuchi H. Lattice swelling with the selective digestion of elastic components in single-skinned fibers from frog muscle. Biophysical Journal. 1987;52:29-32.

28. Trombitas K, and Granzier, H. Actin removal from cardiac myocytes shows that near Z line titin attaches to actin while under tension. Am J Physiol. 1997;273:C662-70.

29. Trombitas K, Jin JP, Granzier H. The mechanically active domain of titin in cardiac muscle. Circ Res. 1995;77:856-61.

30. Millman B., Irving T. Filament lattice of frog striated muscle: radial forces, lattice stability, and filament compression in the A-Band of relaxed and rigor muscle. Biophys. J. 1988;54:437-447.

31. Wakabayashi K. Sugimoto Y., Tanaka H., Ueno Y., Takezawa Y., Amemiya Y. X-ray diffraction evidence for the extensibility of actin and myosin filaments during muscle contraction. Biophysical Journal. 1994;67:2422-2435.

32. Malinchik S, Xu S., and Yu, LC. Temperature-induced structural changes in the myosin thick filament of skinned rabbit psoas muscle. Biophysical Journal. 1997;73:2304-2312.

33. Levine RJ, Yang Z, Epstein ND, Fananapazir L, Stull JT, Sweeney HL. Structural and functional responses of mammalian thick filaments to alterations in myosin regulatory light chains. J Struct Biol. 1998;122:149-61.

34. Weisberg A, Weingrad, S. Alteration of myosin cross bridges by phosphorylation of myosin-binding protein C in cardiac muscle. Proc Natl Acad Sci USA. 1996;93:8999-9003.

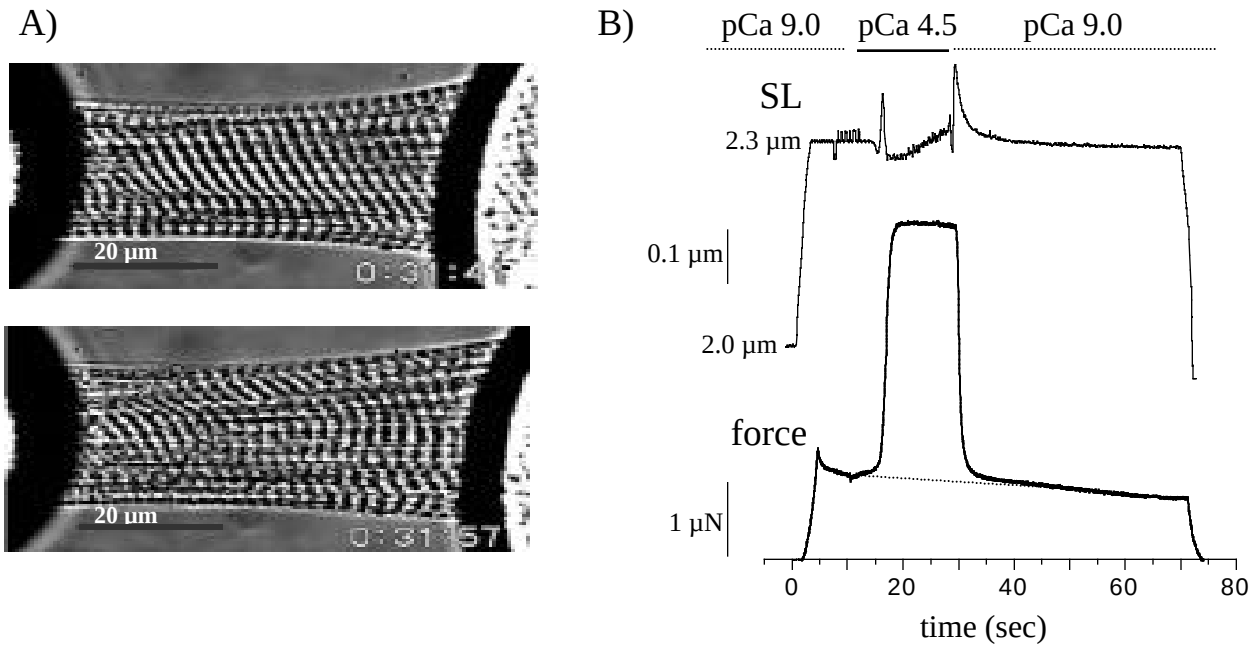
A)
20 µm
20 µm
B)
pCa 9.0
pCa 4.5
pCa 9.0
SL
2.3 µm
0.1 µm
2.0 µm
force
1 µN
0
20
40
60
80
time (sec)

Figure 1.

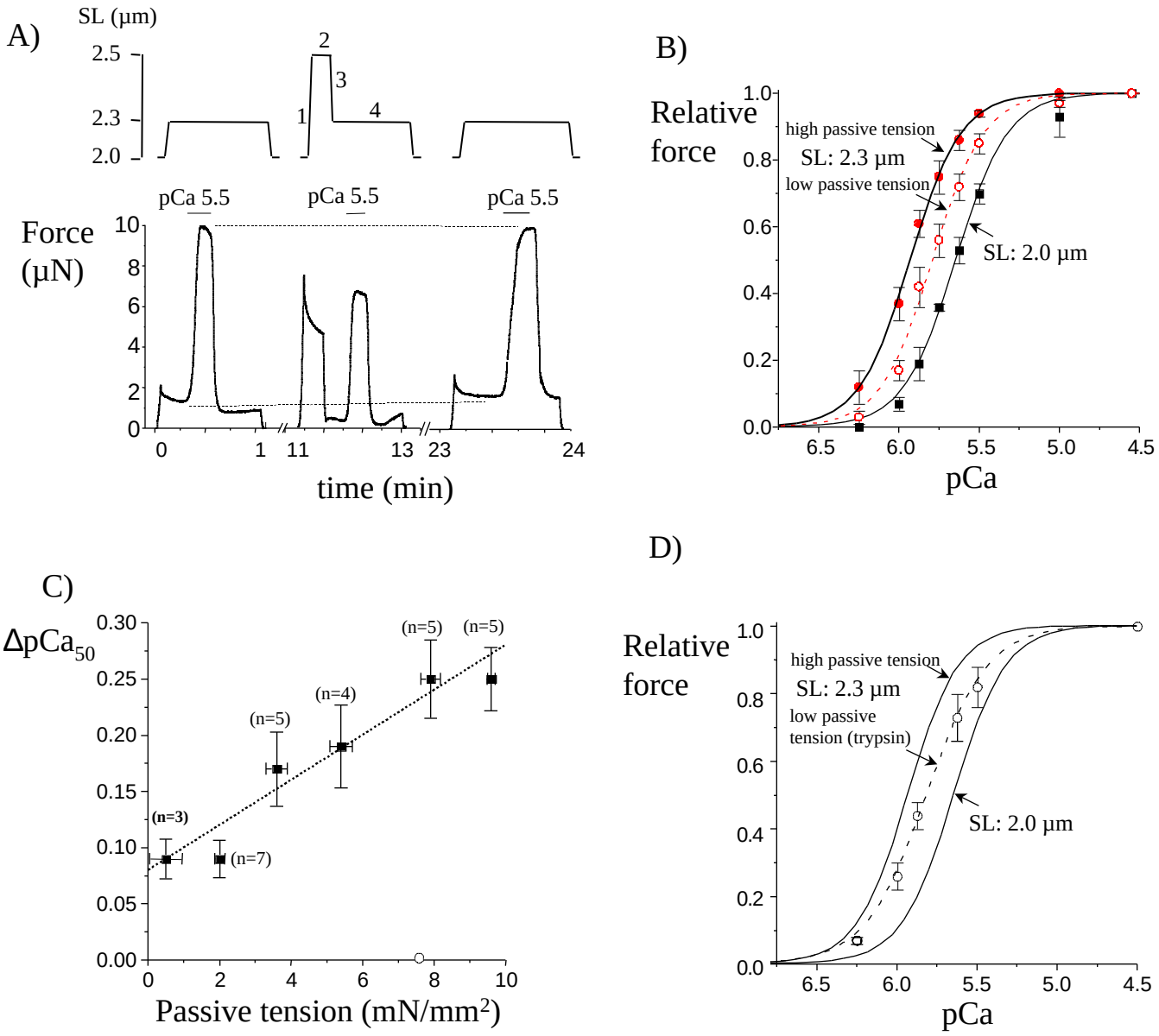
A)
SL (µm)
2.5
2.3
2.0
1
2
3
4
pCa 5.5
pCa 5.5
pCa 5.5
Force (µN)
10
8
6
4
2
0
0
1
11
13
23
24
time (min)
B)
Relative force
high passive tension
SL: 2.3 µm
low passive tension
SL: 2.0 µm
1.0
0.8
0.6
0.4
0.2
0.0
6.5
6.0
5.5
5.0
4.5
pCa
C)
ΔpCa50
0.30
0.25
0.20
0.15
0.10
0.05
0.00
(n=3)
(n=7)
(n=5)
(n=4)
(n=5)
(n=5)
0
2
4
6
8
10
Passive tension (mN/mm2)
D)
Relative force
high passive tension
SL: 2.3 µm
low passive tension (trypsin)
SL: 2.0 µm
1.0
0.8
0.6
0.4
0.2
0.0
6.5
6.0
5.5
5.0
4.5
pCa

Figure 2.

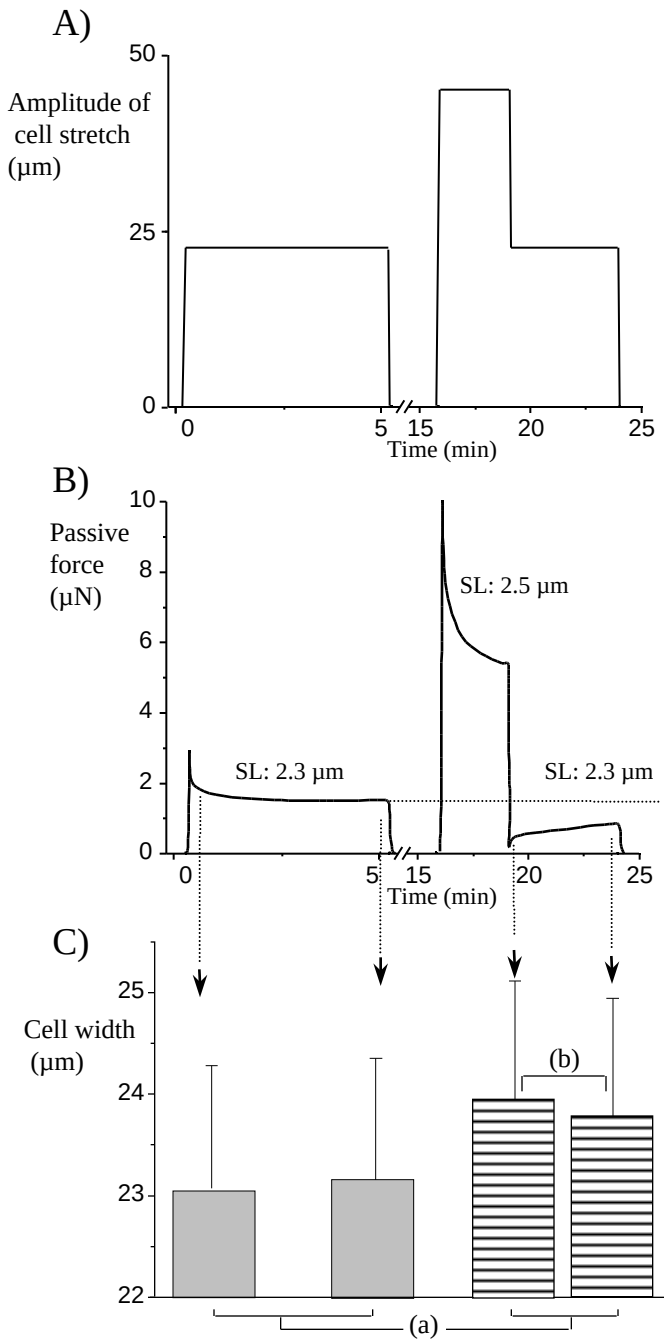
A)
Amplitude of cell stretch (µm)
50
25
0
0
5
15
20
25
Time (min)
B)
Passive force (µN)
10
8
6
4
2
0
SL: 2.5 µm
SL: 2.3 µm
SL: 2.3 µm
0
5
15
20
25
Time (min)
C)
Cell width (µm)
25
24
23
22
(b)
(a)

Figure 3.

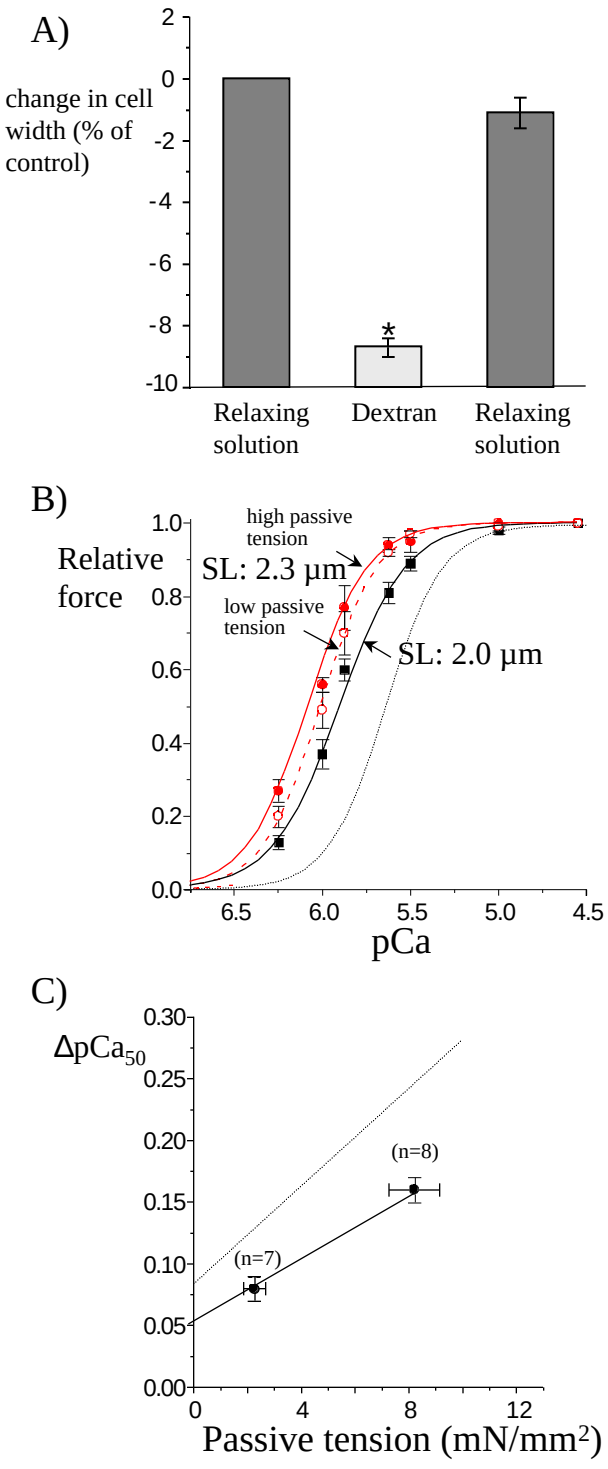
A)
change in cell width (% of control)
2
0
-2
-4
-6
-8
-10
*
Relaxing solution
Dextran
Relaxing solution
B)
Relative force
1.0
0.8
0.6
0.4
0.2
0.0
high passive tension
SL: 2.3 µm
low passive tension
SL: 2.0 µm
6.5
6.0
5.5
5.0
4.5
pCa
C)
ΔpCa50
0.30
0.25
0.20
0.15
0.10
0.05
0.00
(n=8)
(n=7)
0
4
8
12
Passive tension (mN/mm2)

Figure 4.

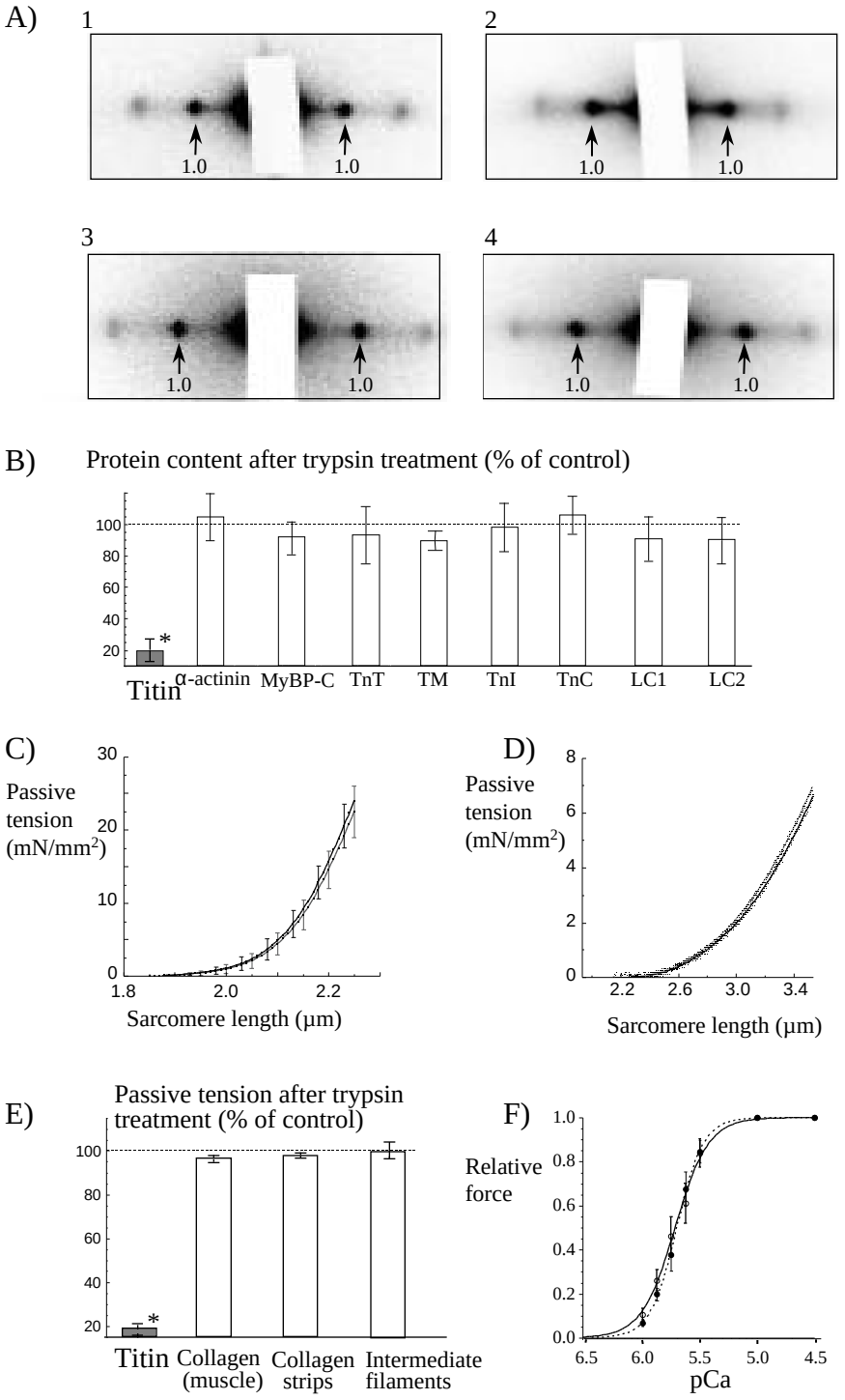
A)
1
2
3
4
1.0
B)
Protein content after trypsin treatment (% of control)
100
80
60
40
20
*
Titin
α-actinin
MyBP-C
TnT
TM
TnI
TnC
LC1
LC2
C)
Passive tension (mN/mm2)
30
20
10
0
1.8
2.0
2.2
Sarcomere length (μm)
D)
Passive tension (mN/mm2)
8
6
4
2
0
2.2
2.6
3.0
3.4
Sarcomere length (μm)
E)
Passive tension after trypsin treatment (% of control)
100
80
60
40
20
*
Titin
Collagen (muscle)
Collagen strips
Intermediate filaments
F)
Relative force
1.0
0.8
0.6
0.4
0.2
0.0
6.5
6.0
5.5
5.0
4.5
pCa

Figure 5.

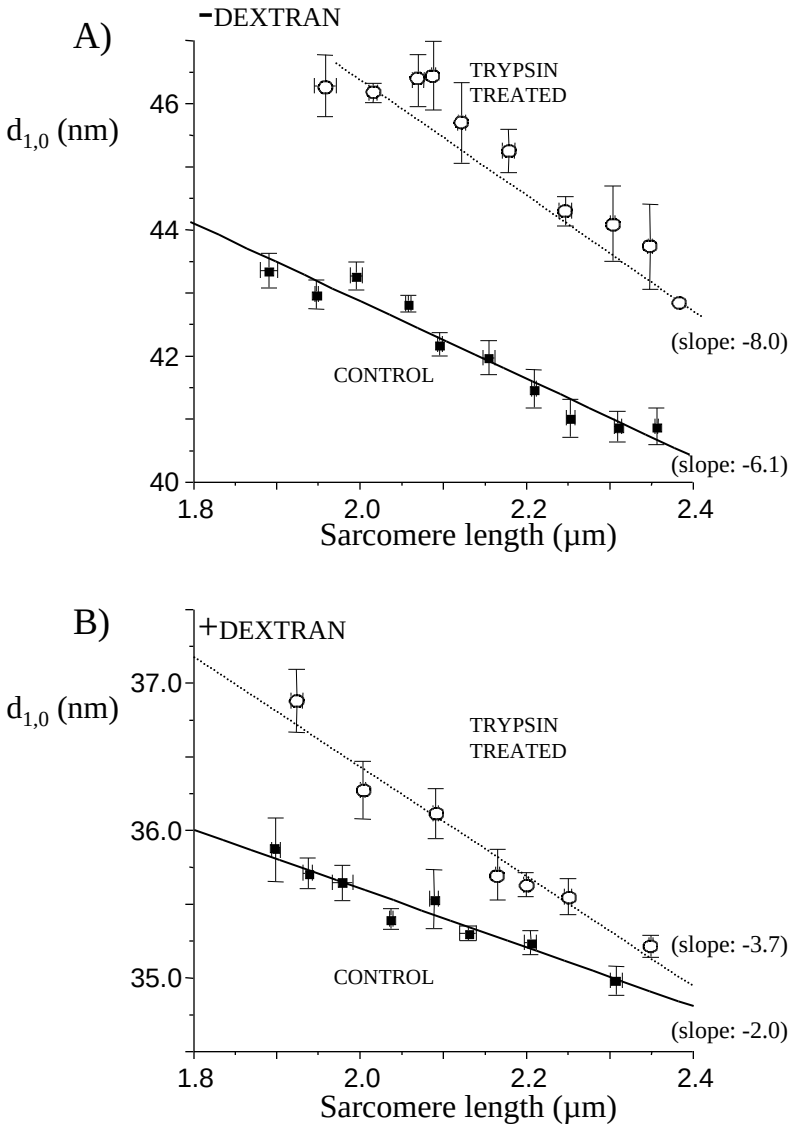
A)
-DEXTRAN
$d_{1,0}$ (nm)
TRYPSIN
TREATED
(slope: -8.0)
CONTROL
(slope: -6.1)
46
44
42
40
1.8
2.0
2.2
2.4
Sarcomere length (μm)
B)
+DEXTRAN
$d_{1,0}$ (nm)
37.0
36.0
35.0
TRYPSIN
TREATED
(slope: -3.7)
CONTROL
(slope: -2.0)
1.8
2.0
2.2
2.4
Sarcomere length (μm)

Figure 6.

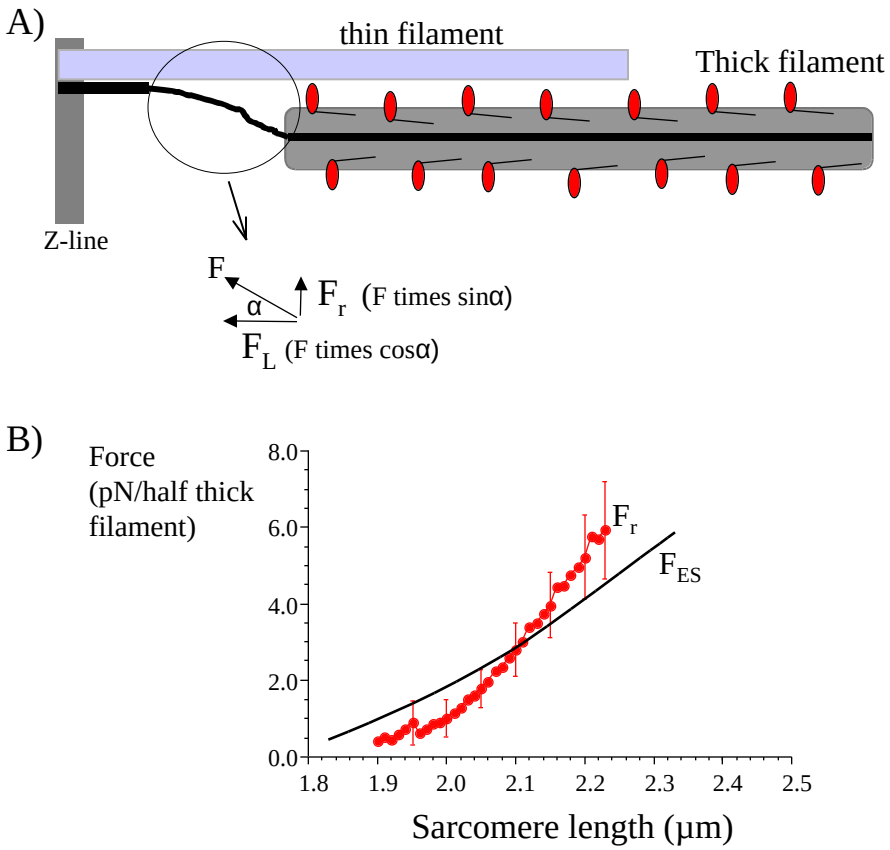
A)
thin filament
Thick filament
Z-line
F
α
F_r (F times sinα)
F_L (F times cosα)
B)
Force
(pN/half thick
filament)
8.0
6.0
4.0
2.0
0.0
1.8
1.9
2.0
2.1
2.2
2.3
2.4
2.5
F_r
F_ES
Sarcomere length (μm)

Figure 7.